70-Year Trends in Ship-Reported Oceanic Precipitation Frequency

Grant W. Petty[1], **Harrison K. Tran**[1]

[1]Atmospheric and Oceanic Sciences Department, University of Wisconsin-Madison

Key Points:

- Significant long-term trends are found in ship reports of precipitation occurrence.
- Trends are mostly positive equatorward of 45° and negative at higher latitudes.
- Reporting biases that could explain the trends cannot be ruled out but have not been identified.

Corresponding author: Grant W. Petty, gwpetty@wisc.edu

Abstract

Ship present-weather reports from 1950 through 2019 are used to assess trends in the reporting of precipitation occurrence over the global oceans. Annual reported precipitation frequency shows statistically significant positive trends of up to ∼15% per decade throughout most ocean areas equatorward of 45 degrees. However, latitudes poleward of 45 degrees are dominated by negative trends, some areas of which meet the 95% confidence threshold. Nine smaller regions were subjectively selected for further investigation, revealing that the observed trends, both positive and negative, are often but not always nearly linear, with the amplitude of interannual fluctuations usually being much larger than that expected from random sampling error alone. The annual time series reveal that four comparatively dry areas are associated with the largest overall positive trends, ranging from 8.3% to 12.8% (relative) per decade. Trends were also computed separately for each season, revealing remarkable overall consistency in trends across seasons.

1 Introduction

In recent years, calibrated satellite measurements have improved our understanding of global precipitation distribution and seasonal evolution, including that of ocean precipitation (Skofronick-Jackson et al., 2017). However, assessing long-term trends in oceanic precipitation remains challenging due in part to the comparatively short and heterogeneous satellite record (Nicolas & Bromwich, 2011). This is particularly true prior to the advent of operational passive microwave imagers in 1987 as well as up to the present at higher latitudes, where microwave sensors may miss shallower, lighter, and especially frozen precipitation (Panegrossi et al., 2022).

Gu and Adler (2022) have undertaken an analysis of trends in precipitation amount covering the 42-year period from 1979 to 2020. Based on the Global Precipitation Climatology Project (GPCP) precipitation product (Adler et al., 2018), their findings reveal a generally weak but statistically significant long-term trend in global mean precipitation. On regional scales, both positive and negative trends have been observed, but statistical significance could not be established.

Non-satellite-based attempts to estimate climatological oceanic precipitation have of necessity relied on subjective and qualitative reports of precipitation occurrence and

type submitted by sparsely and unevenly distributed commercial and military vessels. Researchers produced climatologies of monthly precipitation amounts by assigning nominal intensities to each common present-weather code and aggregating ship reports over time (Tucker, 1961; Reed, 1979; Dorman & Bourke, 1979; Legates & Willmott, 1990). Island weather stations believed to be representative of open-ocean conditions have also been utilized to estimate ocean precipitation amounts (Morrissey et al., 1995), but these are primarily found in atolls in the western tropical Pacific, leaving the vast majority of the global oceans without quantitative measurements.

Sidestepping the challenge of estimating rainfall amount from categorical ship weather reports, Petty (1995) derived a global climatology of ocean precipitation frequency, also known as fractional time precipitating, and precipitation characteristics from 34 years of synoptic ship present-weather reports spanning the period 1958 to 1991. While the categorization of precipitation type and intensity in these reports is inherently subjective, the determination of whether or not it is precipitating is far less so. The study aimed to evaluate satellite-based determinations of simple precipitation occurrence and to elucidate regional and seasonal variations in precipitation properties that could introduce biases into satellite retrievals of rainfall amount. The high-latitude ocean precipitation frequencies derived by Petty (1995) were in sharp contrast with the lower passive microwave-derived estimates of that era (Petty, 1997), but were later largely corroborated by CloudSat observations (Ellis et al., 2009).

Here we take a first step toward updating and extending the previous analysis by examining trends in precipitation frequency over the 70-year time period from 1950 to 2019. This effort is motivated in part by model projections of changes in precipitation amount and distribution in response to climate change (Trenberth, 1999; Chou et al., 2012). One must distinguish, however, between precipitation amount and precipitation frequency, as the former is the product of precipitation frequency with the mean nonzero precipitation rate, which may itself change in a changing climate (Bichet & Diedhiou, 2018). Also, determinations of precipitation frequency are sensitive to the temporal window employed—e.g., instantaneous, hourly, daily, etc. (Trenberth & Zhang, 2018). The precipitation frequency examined herein reflects human observations of sky and weather typically lasting less than 10 minutes and is unlikely to differ much from instantaneous determinations except perhaps where extremely intermittent showery precipitation prevails.

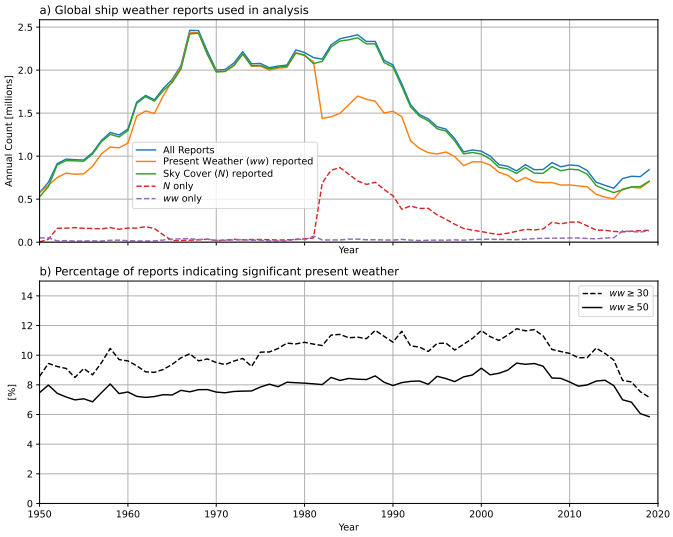

Figure 1. a) Gross annual counts and selected subsets of ship weather reports utilized in the analysis. b) Percentage of reports of significant present-weather ($ww \geq 30$) and of precipitation ($ww \geq 50$) relative to all reports with non-missing sky cover reports N.

2 Data

2.1 Source

We used the latest version of the International Comprehensive Ocean-Atmosphere Data Set (ICOADS) Release 3, Individual Observations (Freeman et al., 2017), which is available through 2019 and continues to be updated. Although this data set includes everything from manned vessels and buoys to autonomous profiling devices and tide gauges, the specific platform types associated with human observations of present-weather include "U.S. Navy" (22.1 million reports, 1950–2019), "merchant/foreign ship" (2.9 million), "ocean station vessel – off station" (0.5 million), "ocean station vessel – on station" (0.9 million), "lightship" (1.0 million), and, the largest category, generic "ship" (100.9 million).

Of the above platform types, only reports from type "ship" are available without interruption throughout the period of interest. Reports identified as "U.S. Navy" are the most numerous type during the first decade of the period but abruptly disappear from the record starting in about 1978, only to reappear in moderate numbers after 2004. Reports from "merchant/foreign ship" comprise about 2.5% of the total and are also un-

evenly distributed through the record. Because U.S. Navy ships are known to have continued transmitting weather reports during years where they do not appear as such in the ICOADS record (the first author was a Navy shipboard weather observer from 1978–1980) and because there was no sudden drop in the total annual report count from all sources, we surmise that Navy reports were tagged as platform type "ship" during the missing period. We ultimately elected to utilize the above three platform types in our analysis, reserving ocean station vessels for possible future use as independent validation at those stations' locations.

Of the 126 million initially qualifying reports, about 1.1 million, or slightly less than 1%, are traceable to the tuna fishing fleet of the Inter-American Tropical Tuna Commission (IATTC) between 1972–1997 (Smith et al., 2016). These observations, contained in ICOADS deck 667, are mostly found in the eastern tropical Pacific Ocean (Worley et al., 1992) but are usually concentrated in small regions that move about from year to year, presumably following tuna populations. We found that these observations introduced large temporal and spatial inhomogeneities in both sampling density and reported precipitation frequency, almost always in otherwise data-sparse areas. A previous study by Woodruff (1995) attributed a bias towards weaker winds within the IATTC data to fair weather bias and excluded IATTC data from published enhanced statistics concerning winds for COADS Release 1a. IATTC data continues to be selectively excluded from COADS Monthly Summary Group products due to these apparent biases (ICOADS, 2016). For similar reasons, as discussed by Freeman et al. (2017), ICOADS observations associated with the Russian Marine Meteorological Data Set (MORMET; deck 732, 7.5 million observations, or about 7% of the total) were excluded from the analysis due to their introduction of large temporal and spatial inhomogeneities.

2.2 Interpretation and quality control

The human-observed present-weather code *ww* is the primary element of interest in ship synoptic reports, typically taken every 3 or 6 hours. The codes 30 and greater describe "significant" present weather at the location of the station and time of the observation, as distinct from phenomena observed from a distance or during the previous hour. Codes 50 and higher refer to various manifestations of precipitation, with 50−59 being drizzle, 60−69 continuous or intermittent rain, 70−79 frozen precipitation, 80−89 showery precipitation, and 90−99 thunderstorms in progress (Petty, 1995). Any value

of 50 or higher is thus treated as human observation of precipitation, while all other values are associated with other weather phenomena. Because precipitation takes priority over other possible present-weather elements, a *ww* code value less than 50 rules out the occurrence of precipitation at the time of the observation.

After 1 January 1982, a rule change allowed synoptic reports to omit the *ww* code if there was no significant weather to report (Dai, 2001). This rule change also introduced the station/weather indicator code *ix*, which discriminated between manned and automated observations (excluded here) and whether or not *ww* was omitted due to a lack of significant weather or rather due to a lack of data. However, evident inconsistencies in the reporting of the *ix* flag precluded its use as the means to distinguish between missing *ww* and lack of significant present weather. Instead, we interpreted the appearance of non-missing present-weather *ww* or sky cover N in a report as evidence that a human observer had made a sky and present-weather observation, in which case missing *ww* likely implied no significant weather.

The final dataset contained 103.7 million reports after applying platform type and deck exclusions as well as the test for non-missing *ww* or N. This total is equivalent to an average of 507 ships reporting every 3 hours over the 70-year record. The annual report counts are depicted in Fig. 1a, including the total (top curve) as well as subsets broken out according to whether N and/or *ww* were reported. There are clearly large variations in both the total number of reports available and in the proportions of different subsets.

To assess whether these obvious heterogeneities might spill over into computed precipitation frequencies, we examined the global percentage of *ww* reports with values of 30 or greater (significant present weather) and 50 or greater (precipitation at the time of the observation). Both fractions are free of large fluctuations over most of the record (Fig. 1b) but exhibit a positive trend of approximately 4.5% (relative) per decade until about 2007, after which there is a rather sharp fall-off in both fractions. The latter period coincides with a marked low point in the overall availability of reports, and it remains unclear pending further investigation whether the decline in apparent significant weather frequency reflects a new reporting bias or rather a shift in the geographic distribution of available reports. Changes in local and regional reported precipitation fre-

quency discussed below should be viewed with caution after 2007, especially if inconsistent with the previous 58 years.

2.3 Potential biases and sampling limitations

Potentially more problematic are inconsistencies or biases in operational procedures, especially those that might change over the 70-year record. For example, a fair-weather bias can arise if ships change course to avoid storms, while a foul-weather bias can occur if weather reports are only submitted when weather is deemed significant. There may also be differences in reporting practices between merchant and military vessels and between crews with varying levels of commitment to World Meteorological Organization reporting standards. It is important to note that shipboard synoptic observations were historically taken to support near-real-time weather analyses of otherwise data-sparse ocean areas and not with long-term climatological applications in mind.

For the present purpose, the most significant reporting biases would be those that change over time. However, any such evolution not tied to documented rule changes would be challenging to identify. Therefore, this study relies on less direct evidence of reporting consistency, such as the temporal and/or spatial coherence of computed trends.

Sampling is the single most critical limitation. Figure 2a depicts the total number of included ship reports per 5-degree latitude/longitude gridbox over the entire period. While heavily traveled areas of the north Pacific and Atlantic oceans have frequent reports, reports are scarce over most of the extratropical southern oceans. Figure 2b depicts total counts of precipitation-only reports ($ww \geq 50$) , which is the figure most relevant to estimating precipitation frequency. In dry regions where precipitation reports are rare, determining trends can be difficult even if reports are common overall.

2.4 Mean precipitation frequency

Figure 2c depicts the ratio of the precipitation counts in Figure 2b to the report counts in Figure 2a, thus providing a gross (and seasonally biased) depiction of overall precipitation frequency. The magnitudes and spatial patterns are remarkably similar to those derived by Ellis et al. (2009) (their Fig. 3a) using CloudSat observations over a one-year period (August 2006 through July 2007). That such dissimilar data sources and time periods nevertheless yield nearly indistinguishable large-scale distributions of ocean

precipitation frequency strengthens the case for the validity of the ship data set for trend analysis.

3 Methods

Ship reports were tabulated at 1-degree and monthly resolution to obtain the number of precipitation reports M and total reports N. These initial gridded maps of M and N were then further aggregated over 3-month seasons and coarser spatial resolutions of 3°, 5°, 7°, 9°, and 11° latitude and longitude, as well as a coarsest spatial resolution of 13° latitude by 26° longitude.

The determination of an unbiased estimate $\hat{f}$ of the unknown true fraction f of precipitation from M and N, along with associated sampling uncertainty, is less trivial than commonly assumed. In particular, for small M, the ratio M/N systematically underestimates the true fraction f for any $f > 0$. While analytic treatments of this problem exist, we opted to use a Monte Carlo-generated lookup table to obtain an unbiased estimate of not only f but also the sampling uncertainty σ as functions of M and N, given an *a priori* uniform distribution of f from 0 to 20%. For large M, $\hat{f} \to M/N$ and $\sigma \to \sqrt{M}/N$.

Starting with the coarsest resolution, the estimates $\hat{f}$ and σ for each 1° gridbox were progressively replaced with results from the next finer resolution if and only if sampling at the new resolution was sufficient to avoid degrading the relative uncertainty $\sigma/\hat{f}$. This compositing approach results in final seasonal and annual maps of $\hat{f}$ and associated σ that are based on coarser-resolution aggregations of reports in data-sparse regions but finer resolution within heavily sampled shipping lanes.

For trend determination, we utilized ordinary least-squares regression (OLS). A two-tailed Student's t-test with 95% confidence level was used to assess the significance of the trends relative to the null hypothesis of zero trend (Fig. 3b). To account for temporal autocorrelation, the effective independent sample size N' assumed for the t-test at each location was reduced to $N' = N(1 - r)/(1 + r)$, where $N = 70$ and r is the lag-1 autocorrelation (Box et al., 2015).

4 Results

4.1 Trends in Annual Precipitation Fraction

Annual trends expressed in percent per decade relative to the mean reported precipitation frequency over the entire period are depicted in Fig. 3a along with areas for which the trend is different from zero with 95% confidence ($p < 0.05$) in Fig. 3b. The result is a remarkably coherent pattern of large, statistically significant positive trends throughout most ocean areas equatorward of 45°. Maximum positive trends exceed 10% per decade in many areas and approach 15% for portions of the south central Atlantic.

Within the same latitude zone, limited areas of negative trend are seen only over the northwestern Pacific, in the general vicinity of Australia, and within the dry zones just off the west coast of African, near 15°N and 15°S, as well as near 5°S off the Peruvian coast. However, most of these areas of negative trend do not meet the chosen significance threshold except in the vicinities of Japan and New Zealand.

Latitudes poleward of 45° are dominated by negative trends, some areas of which meet the significance threshold. The latter include much of the North Atlantic and parts of the Barents Sea.

Irrespective of the locally computed p-value for the trends, the high degree of spatial coherence of both positive and negative trends speaks against these being the result of statistical flukes due to sampling noise. While spurious trends could potentially result from variable seasonal patterns of ship traffic, it is seems unlikely that this mechanism could give rise to trends of similar sign and magnitude over such extensive contiguous areas.

4.2 Annual and seasonal trends in selected areas

Nine smaller regions were subjectively selected for further investigation, as indicated by the dashed boxes in Figs. 2 and 3. The specific box locations were influenced in part by the existence of locally higher sample densities, though"Niño 3.4" (5°S–5°N, 120°W–170°W) was chosen for its association with the El Niño-Southern Oscillation (ENSO) (Barnston, 1997).

4.2.1 Time series of annual frequencies

Time series of the annually aggregated data are depicted as solid curves in Fig. 4. For comparison, the random sampling error σ is shown as dashed curves. Plots are annotated with the means, trends, and p-values. In addition, both annual and seasonal trends are reported in Table 1, with trends passing the significance test highlighted in bold.

The time series reveal that the observed trends, both positive and negative, are often but not always quasi-linear, with the amplitude of interannual fluctuations often being considerably larger than that expected from random sampling error alone. Comparatively rain-free areas ($\bar{f} \leq 0.04$)—Niño 3.4, the Gulf of Mexico, the Arabian Sea, and the southeast Atlantic off the coast of southern Africa (Fig. 4a, c, h, and i, respectively)—are associated with largest overall positive trends, ranging from 8.3% to 12.8% per decade. In particular, the reported frequency of precipitation over in the southeast Atlantic box averaged around 1.5% between 1950 and 1970 but then doubled to an average of about 3% after 2000.

A long-term positive trend is apparent in the Niño 3.4 region along the tropical central Pacific (Fig. 4a). Large peaks in precipitation frequency appear to correspond with El Niño events such as in 1982–83, 1997–98, and 2015–16, while deficits in precipitation frequency appear to correspond with La Niña events such as in 1988–89 and 1998-99. The general correspondence of this time series with well-documented ENSO activity lends further confidence in the ship record for examining precipitation variability.

In the western tropical Pacific (Fig. 4e), an overall linear trend is less apparent; rather, the frequency averages around 6.5% in the first decade, is flat or even slightly decreasing with a mean of around 8% until 1990, and then increasing fairly sharply to an average of over 10% during 2009–2014 before falling off again. Similarly, in the Southern Pacific Convergence Zone (SPCZ; Fig. 4f), there is a general downward trend until the mid-1980s followed by a positive trend ending with a large jump in 2014. The latter jump coincides with a much smaller-than-normal sample size for that year, so that feature may not be reliable.

Significant negative trends of 3.0% and 2.4% per decade are seen in the north Atlantic (Fig. 4b) and near the Sea of Okhotsk (Fig. 4g), respectively. In the former case, the trend is relatively flat until about 2005, after which the precipitation frequency drops

Table 1. Trends in precipitation frequency for the indicated focus areas, expressed as the percent change per decade relative to the mean for the 70-year period. Results are given for annual reports and for the indicated 3-month seasons. Bolded values are significant at the 95% confidence level.

Region	Latitude	Longitude	Annual	MAM	JJA	SON	DJF
Niño 3.4	5S–5N	170W–120W	**+9.4**	**+9.5**	**+9.3**	+6.0	**+9.5**
North Atlantic	45N–60N	45W–30W	**−3.0**	**−3.2**	**−2.5**	**−3.1**	−1.8
Gulf of Mexico	15N–30N	95W–80W	**+10.2**	**+7.4**	**+12.5**	**+11.1**	**+9.1**
Tropical Atlantic	5S–10N	45W–30W	**+9.9**	**+8.9**	**+10.1**	**+9.8**	**+11.4**
West. Trop. Pacific	5S–15N	120E–155E	**+5.1**	**+6.9**	**+4.5**	**+2.3**	**+6.5**
S. Pac. Conv. Zone	30S–15S	180W–150W	**+3.6**	+5.4	+2.8	+2.2	+2.8
Sea of Okhotsk	40N–55N	145E–160E	**−2.4**	**−2.7**	**−4.9**	**−3.5**	**−2.9**
Arabian Sea	5N–20N	55E–70E	**+8.3**	+3.9	**+13.2**	**+8.1**	+0.2
Southeast Atlantic	35S–20S	0–15E	**+12.8**	**+14.2**	**+15.3**	**+11.0**.	+7.1

by about 2.5% in absolute terms or more than 15% relative to its previous average value of about 16%. It must be noted that the period of largest dropoff roughly coincides with the global drop in the reporting of significant present-weather seen in Fig. 1, so we cannot rule out a reporting bias contributing to the dropoff in Fig. 4b. Hints of similar declines are seen in certain of the other time series, including two with otherwise strong positive trends, such as the Gulf of Mexico (Fig. 4c) and the western tropical Pacific (Fig. 4c).

4.2.2 Trends by season

Within the geographic boxes described above, ship reports were further stratified into 3-month periods—March/April/May (MAM), June/July/August (JJA), September/October/November (SON), and December/January/February (DJF) to permit the determination of trends separately within each season. This also reduces the potential for intraannual sampling biases in the determination of trends. Trends for each period are given in Table 1.

The most striking overall result is that for almost all geographic boxes, not only the sign but also the general magnitude of the trend is similar across all four seasons.

This high degree of consistency appears to rule out statistical sampling error as the source of the apparent trends. It also suggests that whatever meteorological or procedural changes may have occurred over the 70 years, they are not significantly influenced by time of year.

5 Conclusions

Our initial analysis of 70 years of shipboard synoptic weather reports reveals significant positive trends in oceanic precipitation occurrence over broad swaths equatorward of 45° latitude, but predominantly negative at higher latitudes. We have not identified any potential sampling or reporting bias that could give rise to the observed geospatial patterns and general consistency across seasons. Unfortunately, there exists no ocean precipitation dataset both extensive and homogeneous enough to validate our findings globally, though local and regional comparisons may be possible.

If real, the positive trends at lower latitudes are not inconsistent with those expected due to global warming and associated mechanisms (Chou et al., 2012), while negative trends at higher latitudes might be related to reduced open-cell convective precipitation and/or precipitation suppression due to increasing anthropogenic aerosol (Rosenfeld et al., 2006). Further analysis is also needed to assess the relationship between these trends and known interannual and interdecadal climate variations (Gu & Adler, 2013). Finally, ongoing work with this dataset includes assessing trends in the fractions of precipitation due to drizzle, snow, and other subclasses as well as undertaking intercomparisons with ocean station vessels, where available, and with the much shorter record of satellite-derived precipitation.

6 Open Research

ICOADS-3 data are available from Research Data Archive, Computational and Information Systems Laboratory, National Center for Atmospheric Research, University Corporation for Atmospheric Research et al. (2016). Complete Jupyter/Python notebooks used to obtain numerical and graphical results herein are posted at `github.com/gpetty/GRL-2023`.

Acknowledgments

The author thanks Tristan L'Ecuyer for helpful comments on the manuscript. This work was partially supported by the NASA Precipitation Measurement Mission project, Grants NNX16AF70G and 80NSSC22K0601.

References

Adler, R. F., Sapiano, M. R., Huffman, G. J., Wang, J.-J., Gu, G., Bolvin, D., ... others (2018). The Global Precipitation Climatology Project (GPCP) monthly analysis (new version 2.3) and a review of 2017 global precipitation. *Atmosphere*, *9*(4), 138.

Barnston, A. G. (1997). Documentation of a highly ENSO-related SST region in the equatorial Pacific. *Atmosphere-Ocean*, *35*, 367–383.

Bichet, A., & Diedhiou, A. (2018). Less frequent and more intense rainfall along the coast of the gulf of guinea in west and central africa (1981 2014). *Climate Research*, *76*(3), 191–201.

Box, G. E., Jenkins, G. M., Reinsel, G. C., & Ljung, G. M. (2015). *Time Series Analysis: Forecasting and Control*. John Wiley & Sons.

Chou, C., Chen, C.-A., Tan, P.-H., & Chen, K. T. (2012). Mechanisms for global warming impacts on precipitation frequency and intensity. *Journal of Climate*, *25*(9), 3291–3306.

Dai, A. (2001). Global precipitation and thunderstorm frequencies. Part I: Seasonal and interannual variations. *Journal of Climate*, *14*(6), 1092–1111.

Dorman, C. E., & Bourke, R. H. (1979). Precipitation over the Pacific Ocean, 30 S to 60 N. *Monthly Weather Review*, *107*(7), 896–910.

Ellis, T. D., L'Ecuyer, T., Haynes, J. M., & Stephens, G. L. (2009). How often does it rain over the global oceans? The perspective from CloudSat. *Geophysical research letters*, *36*(3).

Freeman, E., Woodruff, S. D., Worley, S. J., Lubker, S. J., Kent, E. C., Angel, W. E., ... others (2017). ICOADS Release 3.0: a major update to the historical marine climate record. *International Journal of Climatology*, *37*(5), 2211–2232.

Gu, G., & Adler, R. F. (2013). Interdecadal variability/long-term changes in global precipitation patterns during the past three decades: global warming and/or

pacific decadal variability? *Climate Dynamics*, *40*, 3009–3022.

Gu, G., & Adler, R. F. (2022). Observed variability and trends in global precipitation during 1979–2020. *Climate Dynamics*, 1–20.

ICOADS. (2016). *International Comprehensive Ocean-Atmosphere Data Set (ICOADS) Release 3.0 Quality Control (QC) and Related Processing (Draft).* https://icoads.noaa.gov/e-doc/R3.0-stat_trim.pdf.

Legates, D. R., & Willmott, C. J. (1990). Mean seasonal and spatial variability in gauge-corrected, global precipitation. *International Journal of Climatology*, *10*(2), 111–127.

Morrissey, M. L., Shafer, M. A., Postawko, S. E., & Gibson, B. (1995). The Pacific rain gage rainfall database. *Water Resources Research*, *31*(8), 2111–2113.

Nicolas, J. P., & Bromwich, D. H. (2011). Precipitation changes in high southern latitudes from global reanalyses: A cautionary tale. *Surveys in Geophysics*, *32*, 475–494.

Panegrossi, G., Casella, D., Sanò, P., Camplani, A., & Battaglia, A. (2022). Recent advances and challenges in satellite-based snowfall detection and estimation. *Precipitation Science*, 333–376.

Petty, G. W. (1995). Frequencies and characteristics of global oceanic precipitation from shipboard present-weather reports. *Bulletin of the American Meteorological Society*, *76*(9), 1593–1616.

Petty, G. W. (1997). An intercomparison of oceanic precipitation frequencies from 10 Special Sensor Microwave/Imager rain rate algorithms and shipboard present weather reports. *Journal of Geophysical Research: Atmospheres*, *102*(D2), 1757–1777.

Reed, R. (1979). On the relationship between the amount and frequency of precipitation over the ocean. *Journal of Applied Meteorology*, *18*(5), 692–696.

Research Data Archive, Computational and Information Systems Laboratory, National Center for Atmospheric Research, University Corporation for Atmospheric Research, Physical Sciences Division, Earth System Research Laboratory, OAR, NOAA, U.S. Department of Commerce, Cooperative Institute for Research in Environmental Sciences, University of Colorado, National Oceanography Centre, University of Southampton, Met Office, Ministry of Defence, United Kingdom, Deutscher Wetterdienst (German Meteorological Ser-

vice), Germany, ... National Centers for Environmental Information, NESDIS, NOAA, U.S. Department of Commerce (2016). *International Comprehensive Ocean-Atmosphere Data Set (ICOADS) Release 3, Individual Observations.* Boulder CO: Research Data Archive at the National Center for Atmospheric Research, Computational and Information Systems Laboratory. Retrieved from `https://doi.org/10.5065/D6ZS2TR3`

Rosenfeld, D., Kaufman, Y., & Koren, I. (2006). Switching cloud cover and dynamical regimes from open to closed benard cells in response to the suppression of precipitation by aerosols. *Atmospheric Chemistry and Physics*, *6*(9), 2503–2511.

Skofronick-Jackson, G., Petersen, W. A., Berg, W., Kidd, C., Stocker, E. F., Kirschbaum, D. B., ... others (2017). The Global Precipitation Measurement (GPM) mission for science and society. *Bulletin of the American Meteorological Society*, *98*(8), 1679–1695.

Smith, S. R., Freeman, E., Lubker, S. J., Woodruff, S. D., Worley, S. J., Angel, W. E., ... Kent, E. C. (2016). *The International Maritime Meteorological Archive (IMMA) Format* (Vol. 3).

Trenberth, K. E. (1999). Conceptual framework for changes of extremes of the hydrological cycle with climate change. *Weather and Climate extremes: Changes, Variations and a Perspective from the Insurance Industry*, 327–339.

Trenberth, K. E., & Zhang, Y. (2018). How often does it really rain? *Bulletin of the American Meteorological Society*, *99*(2), 289–298.

Tucker, G. (1961). Precipitation over the north Atlantic Ocean. *Quarterly Journal of the Royal Meteorological Society*, *87*(372), 147–158.

Woodruff, S. D. (1995). COADS Project report I: update plans and unresolved issues. In *Proceedings of the International COADS Winds Workshop, Kiel, Germany, 31 May-2 June 1994* (pp. 12–28).

Worley, S. J., Diaz, H., Wolter, K., & Woodruff, S. D. (1992). Status of other new data sets for coads. In *Proceedings of the International COADS Workshop, Boulder, Colorado, 13-15 January 1992.*

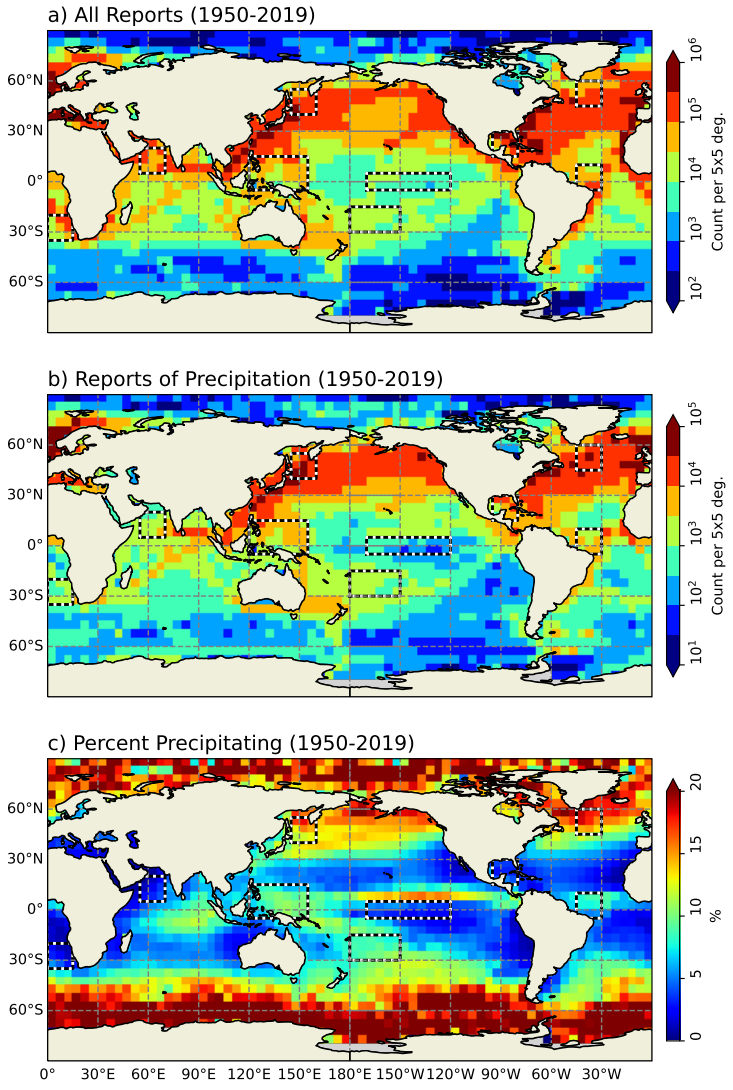

Figure 2. a) Total counts of included ship weather reports ("U.S. Navy", "merchant/foreign ship", and "ship" platform types) per 5°×5° degree box over the 70-year period of interest. b) Counts of reports indicating present precipitation only. c) The ratio of precipitation reports to total reports. Nine dashed boxes depict areas selected for additional analysis.

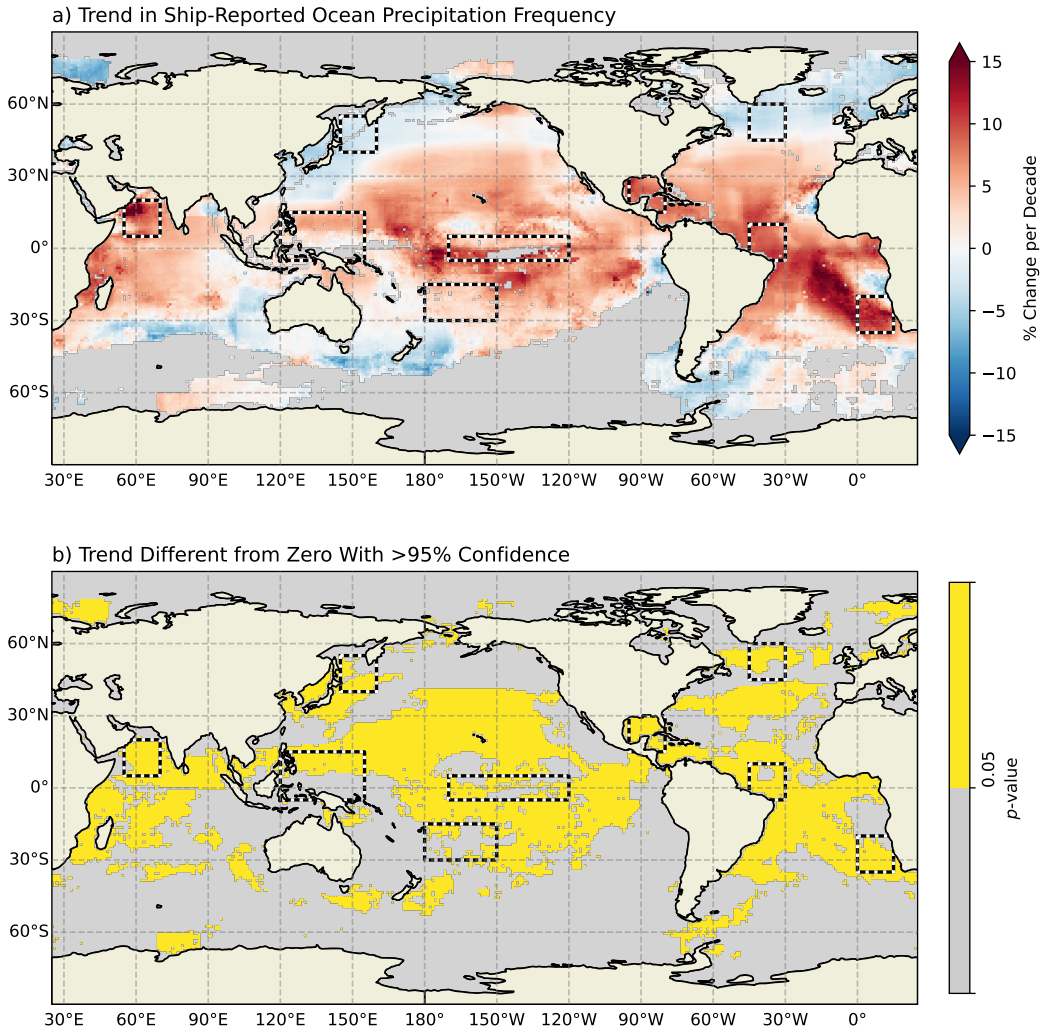

Figure 3. a) Mean trend over 70 years in precipitation frequency computed from ship reports aggregated by year. Trends are expressed as percent changes (relative to the mean precipitation frequency) per decade. Gray regions denote areas lacking the minimum number of ship observations for at least 5 years in the 70-year record. b) Areas with trends different from zero with 95% confidence. Nine dashed boxes depict areas selected for additional analysis.

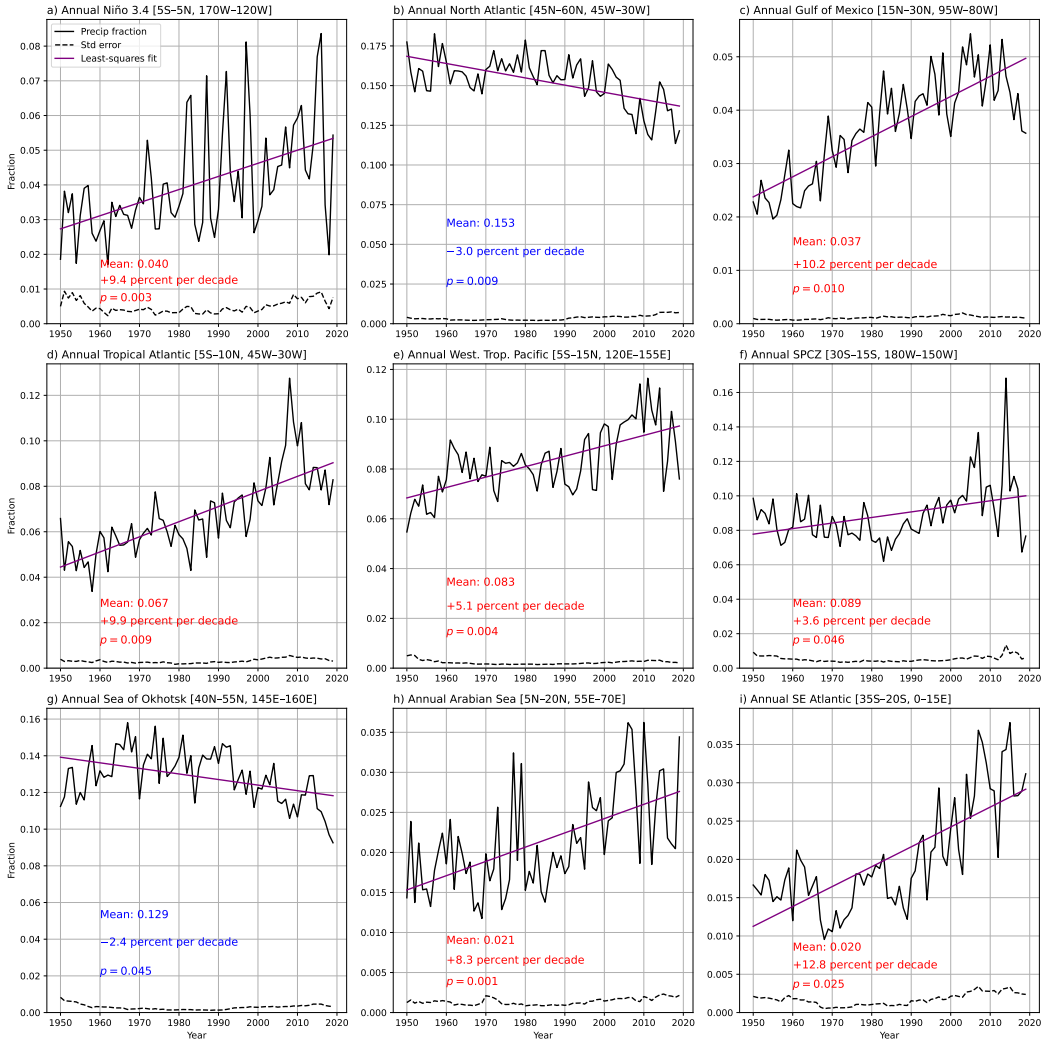

Figure 4. Time series of precipitation frequency computed from yearly ship reports within the indicated latitude/longitude boxes, which correspond to those depicted in Figs. 2 and 3. Dashed lines indicate the random sampling uncertainty.

Figure 1.

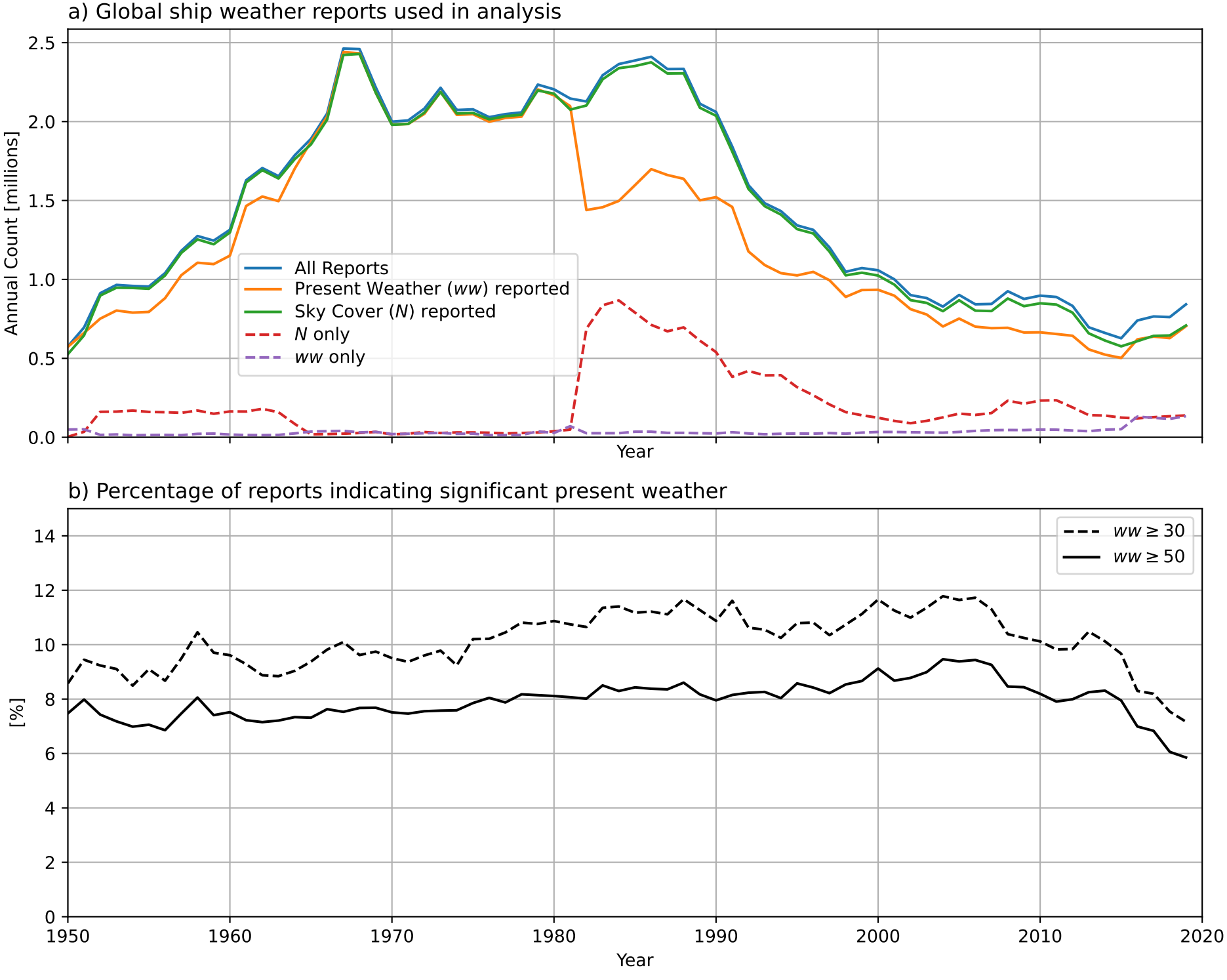
a) Global ship weather reports used in analysis
Annual Count [millions]
2.5
2.0
1.5
1.0
0.5
0.0
All Reports
Present Weather (ww) reported
Sky Cover (N) reported
N only
ww only
Year
b) Percentage of reports indicating significant present weather
[%]
14
12
10
8
6
4
2
0
ww ≥ 30
ww ≥ 50
1950
1960
1970
1980
1990
2000
2010
2020
Year

Figure 2.

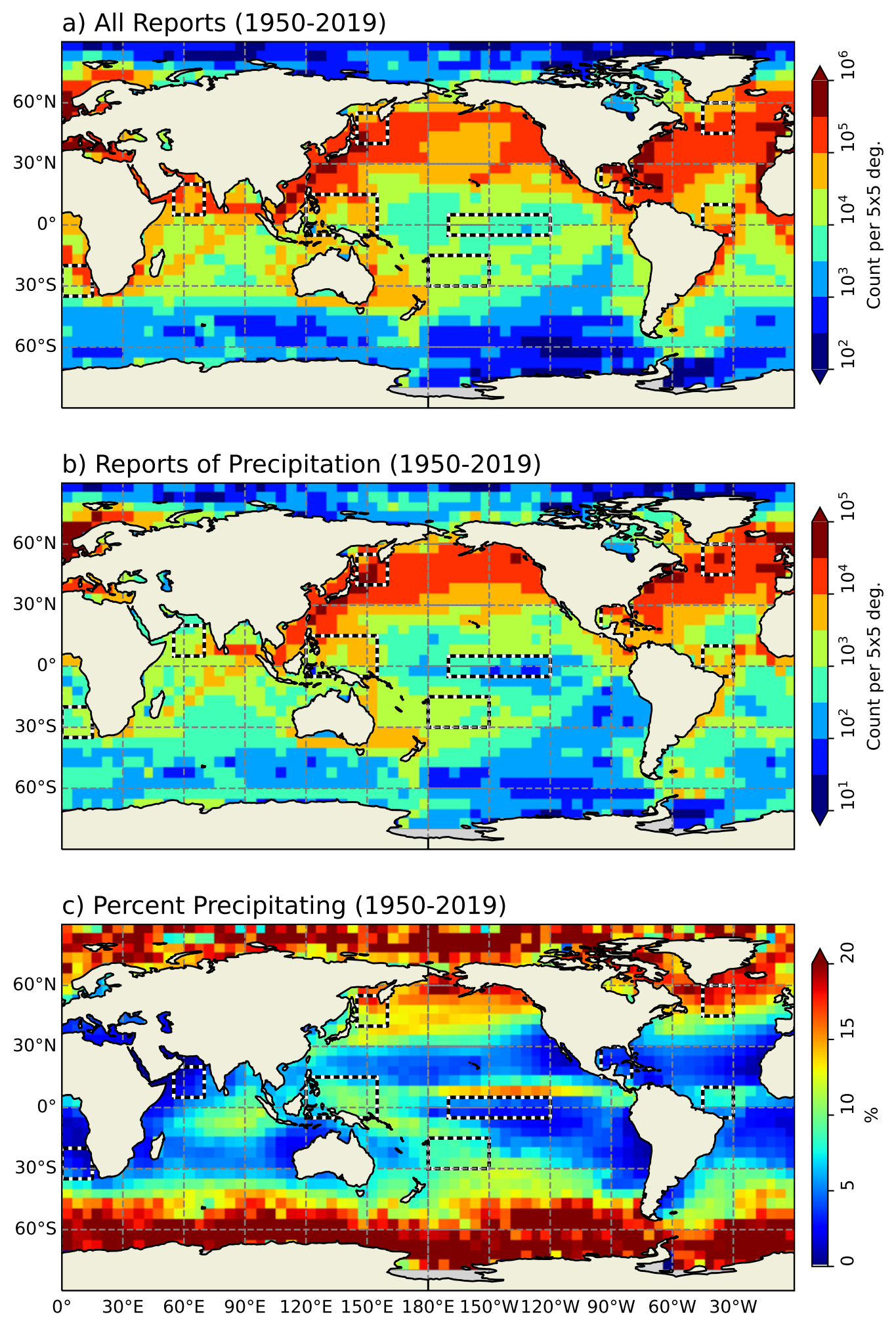
a) All Reports (1950-2019)
b) Reports of Precipitation (1950-2019)
c) Percent Precipitating (1950-2019)
60°N
30°N
0°
30°S
60°S
0°
30°E
60°E
90°E
120°E
150°E
180°E
150°W
120°W
90°W
60°W
30°W
Count per 5x5 deg.
10^2
10^3
10^4
10^5
10^6
10^1
%
0
5
10
15
20

Figure 3.

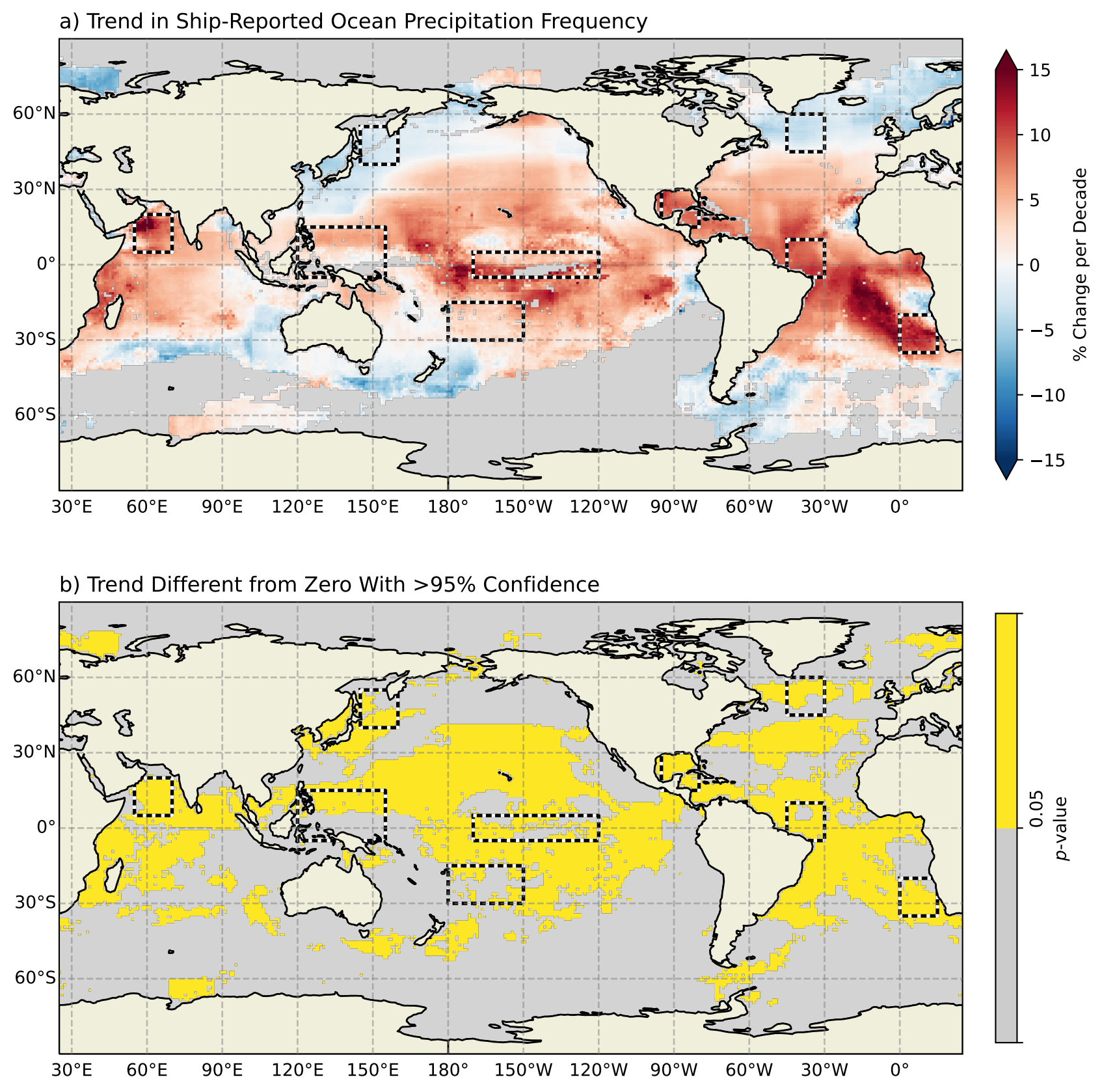
a) Trend in Ship-Reported Ocean Precipitation Frequency
60°N
30°N
0°
30°S
60°S
30°E
60°E
90°E
120°E
150°E
180°
150°W
120°W
90°W
60°W
30°W
0°
15
10
5
0
−5
−10
−15
% Change per Decade
b) Trend Different from Zero With >95% Confidence
60°N
30°N
0°
30°S
60°S
30°E
60°E
90°E
120°E
150°E
180°
150°W
120°W
90°W
60°W
30°W
0°
0.05
p-value

Figure 4.

a) Annual Niño 3.4 [5S–5N, 170W–120W]

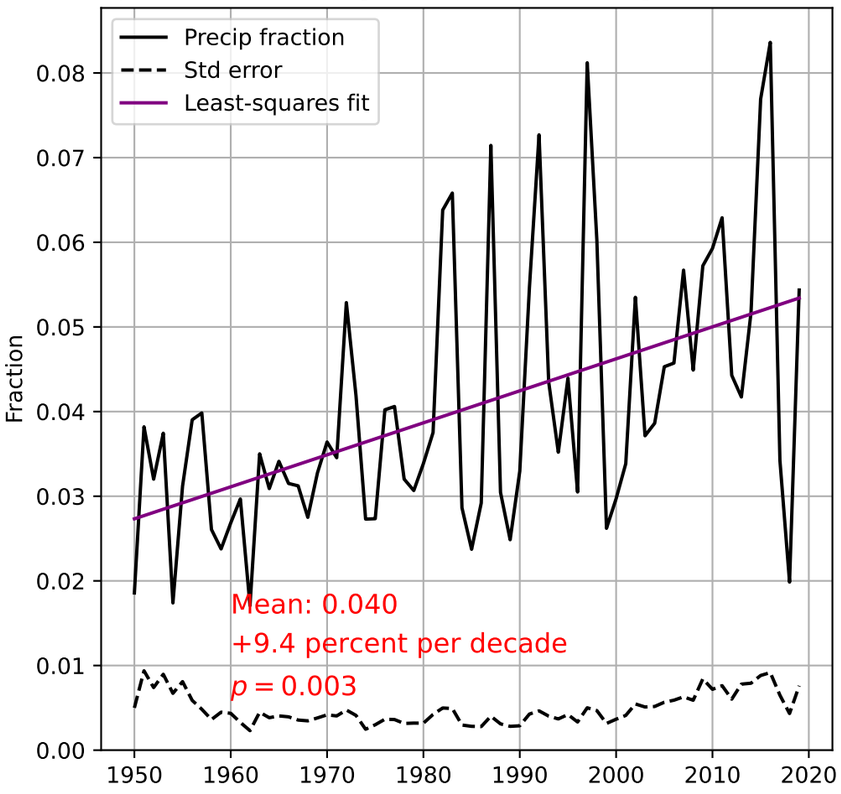

b) Annual North Atlantic [45N–60N, 45W–30W]

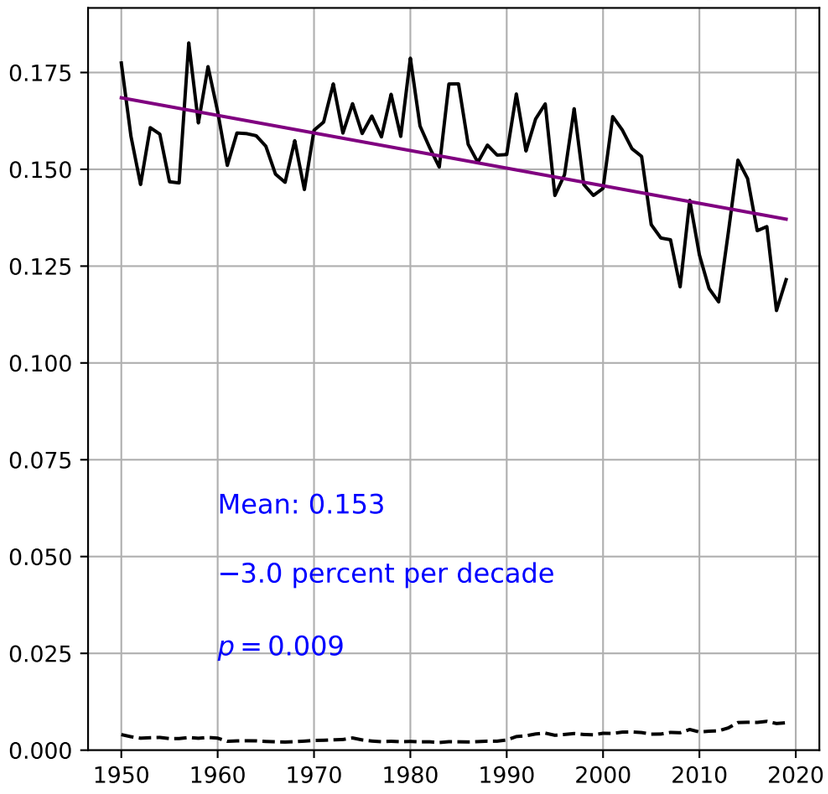

c) Annual Gulf of Mexico [15N–30N, 95W–80W]

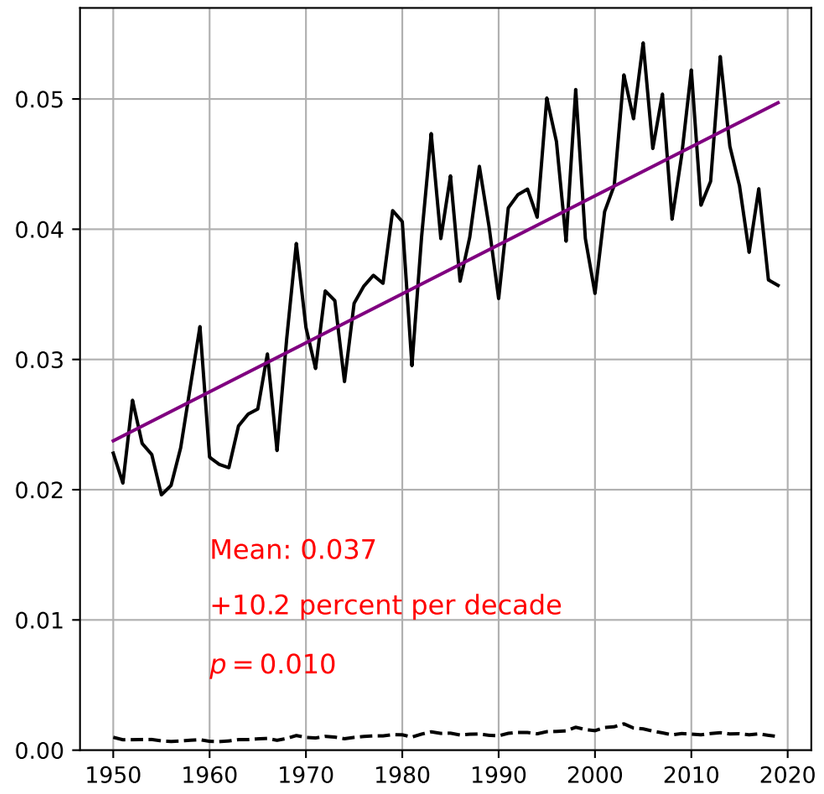

d) Annual Tropical Atlantic [5S–10N, 45W–30W]

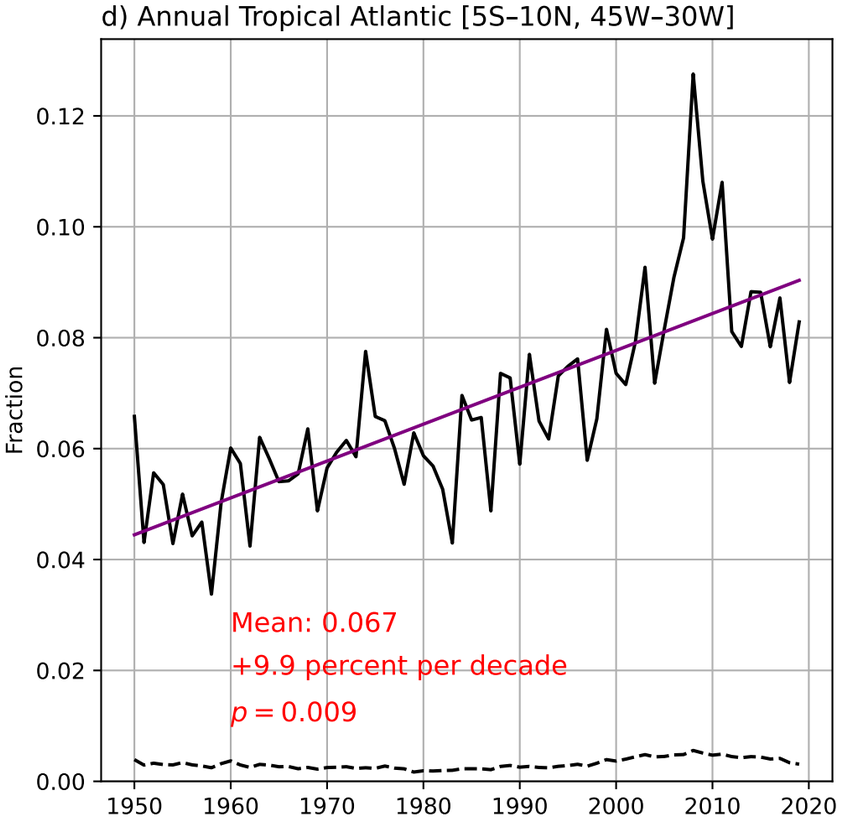

e) Annual West. Trop. Pacific [5S–15N, 120E–155E]

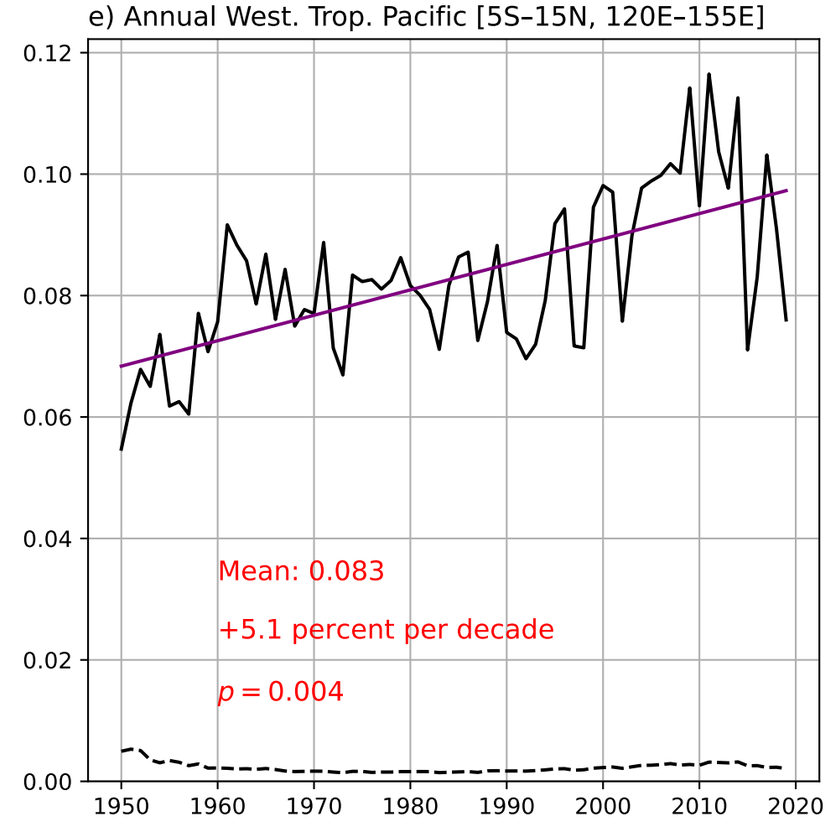

f) Annual SPCZ [30S–15S, 180W–150W]

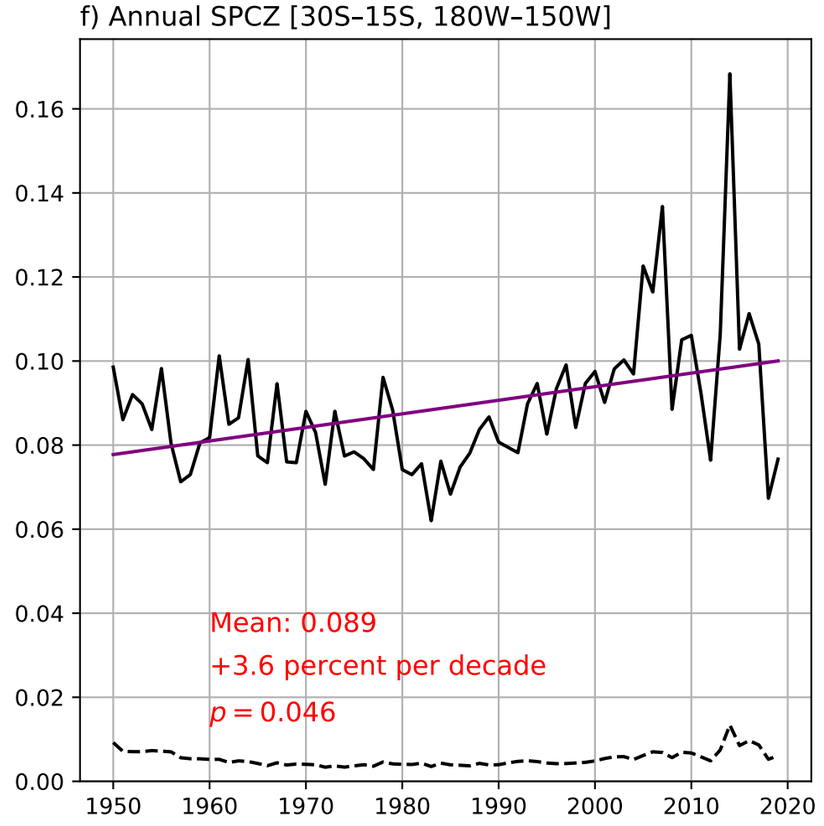

g) Annual Sea of Okhotsk [40N–55N, 145E–160E]

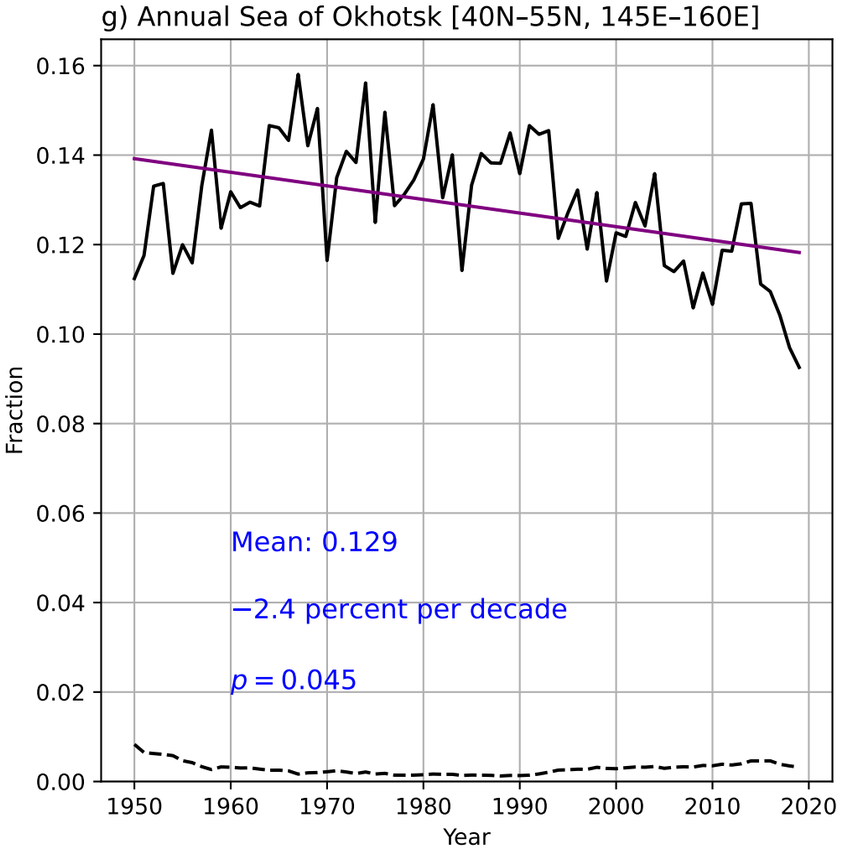

h) Annual Arabian Sea [5N–20N, 55E–70E]

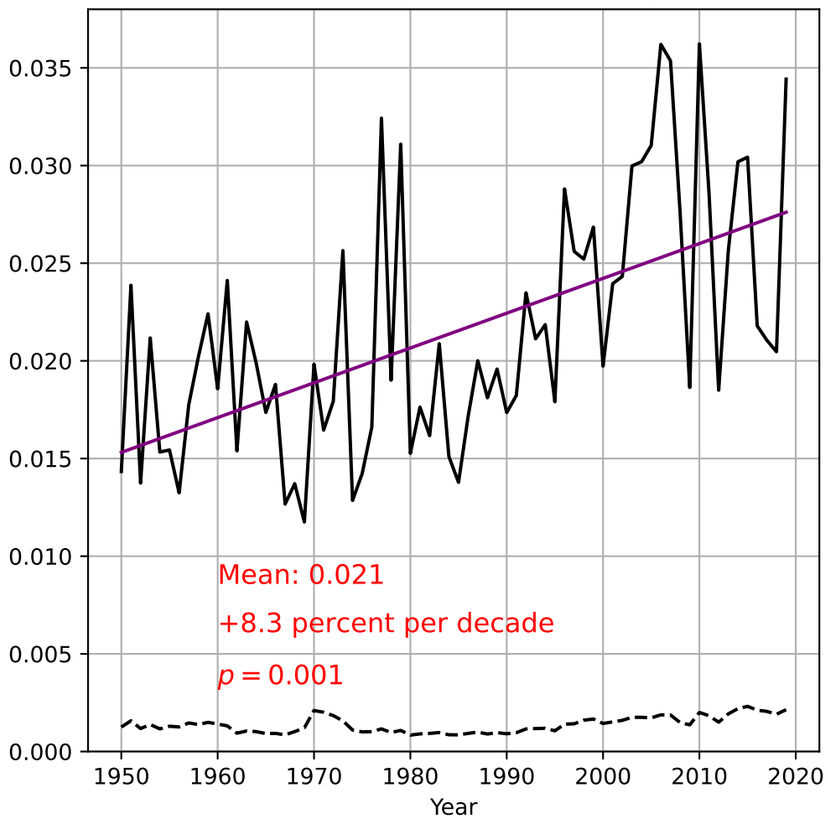

i) Annual SE Atlantic [35S–20S, 0–15E]